Crystalline Ceramic Waste Forms: Report Detailing Data Collection in Support of Potential FY13 Pilot Scale Melter Test

Fuel Cycle Research & Development

Prepared for
U.S. Department of Energy
Separations and Waste Forms
K.S. Brinkman, K.M. Fox, J. Amoroso, and
J.C. Marra
Savannah River National Laboratory
M. Tang
Los Alamos National Laboratory

September 21, 2012
FCRD-SWF-2012-000329
SRNL-STI-2012-00587

Crystalline Ceramic Waste Forms: Report Detailing Data Collection in Support of Potential FY13 Pilot Scale Melter Test

ii   September 21, 2012

Crystalline Ceramic Waste Forms: Report Detailing Data Collection in Support of Potential FY13 Pilot Scale Melter Test

September 21, 2012   v

SUMMARY

The research conducted in this work package is aimed at taking advantage of the long term thermodynamic stability of crystalline ceramics to create more durable waste forms (as compared to high level waste glass) in order to reduce the reliance on engineered and natural barrier systems. Durable ceramic waste forms that incorporate a wide range of radionuclides have the potential to broaden the available disposal options and to lower the storage and disposal costs associated with advanced fuel cycles. Assemblages of several titanate phases have been successfully demonstrated to incorporate radioactive waste elements, and the multiphase nature of these materials allows them to accommodate variation in the waste composition. Recent work has shown that they can be successfully produced from a melting and crystallization process. The objective of this report is to summarize the data collection in support of future melter demonstration testing for crystalline ceramic waste forms.

The waste stream used as the basis for the development and testing is a combination of the projected Cs/Sr separated stream, the Trivalent Actinide - Lanthanide Separation by Phosphorous reagent Extraction from Aqueous Komplexes (TALSPEAK) waste stream consisting of lanthanide fission products, the transition metal fission product waste stream resulting from the transuranic extraction (TRUEX) process, and a high molybdenum concentration with relatively low noble metal concentrations.

The principal difficulties encountered during processing of the "reference ceramic" waste form by a melt and crystallization process were the incomplete incorporation of Cs into the hollandite phase and the presence of secondary Cs-Mo non-durable phases. In the single phase hollandite system, these issues were addressed in this study by refining the compositions to include Cr as a transition metal element and the use of Ti/TiO_2 buffer to maintain reducing conditions. Initial viscosity studies of ceramic waste forms indicated that the pour spout must be maintained above $1400^{\circ}C$ to avoid flow blockages due to crystallization. *In-situ* electron irradiations simulate radiolysis effects indicated hollandite undergoes a crystalline to amorphous transition after a radiation dose of 10^{13} Gy which corresponds to approximately 1000 years at anticipated doses (2×10^{10}-2×10^{11} Gy). Dual-beam ion irradiations employing light ion beam (such as 5 MeV alpha) and heavy ion beam (such as 100 keV Kr) studies indicate that reference ceramic waste forms are radiation tolerant to the β–particles and α-particles, but are susceptible to a crystalline to amorphous transition under recoil nuclei effects.

A path forward for refining the processing steps needed to form the targeted phase assemblages is outlined in this report. Processing modifications including melting in a reducing atmosphere with the use of Ti/TiO_2 buffers, and the addition of Cr to the transition metal additives to facilitate Cs-incorporation in the hollandite phase. In addition to melt processing, alternative fabrication routes are being considered including Spark Plasma Sintering (SPS) and Hot Isostatic Pressing (HIP).

Crystalline Ceramic Waste Forms: Report Detailing Data Collection in Support of Potential FY13 Pilot Scale Melter Test

vi   September 21, 2012

CONTENTS

FIGURES

Crystalline Ceramic Waste Forms: Report Detailing Data Collection in Support of Potential FY13 Pilot Scale Melter Test

viii   September 21, 2012

TABLES

ABBREVIATIONS

AFCI	Advanced Fuel Cycle Initiative
CCIM	Cold Crucible Induction Melter
CS	Cesium/Strontium
DOE	Department of Energy
EDAX	Energy Dispersive Spectroscopy
FCR&D	Fuel Cycle Research and Development
HLW	High Level Waste
LANL	Los Alamos National Laboratory
LN	Lanthanides
NM	Noble Metals
PCT	Product Consistency Test
PUREX	Plutonium, Uranium, Extraction Processes
Redox	Reduction/Oxidation
SEM	Scanning Electron Microscopy
SRNL	Savannah River National Laboratory
SYNROC	Titanium based ceramic substance that can incorporate nuclear waste
TALSPEAK	Trivalent Actinide - Lanthanide Separation by Phosphorous reagent Extraction from Aqueous Komplexes
TEM	Transmission Electron Microscopy
TM	Transition Metals
TRUEX	Transuranic Extraction
XRD	X-ray Diffraction

Crystalline Ceramic Waste Forms: Report Detailing Data Collection in Support of Potential FY13 Pilot Scale Melter Test

x   September 21, 2012

ACKNOWLEDGEMENTS

1.   Introduction

The research conducted by the United States Department of Energy (DOE) under the advanced waste forms division of the FCR&D program is to make the U.S. fuel cycle more effective by developing next generation waste management technologies capable of processing waste material generated from fuel cycle separations for Used Nuclear Fuel (UNF) and from the fabrication of advanced fuels or targets containing materials to be transmuted.[1-3] The research described in this work package was aimed at taking advantage of the long term thermodynamic stability of crystalline ceramics to create more durable waste forms (as compared to high level waste (HLW) glass) in order to broaden the available disposal options and to lower the storage and disposal costs associated with advanced fuel cycles.

Crystalline ceramic waste forms incorporate radionuclides as part of their crystal structure.[4] As such, ceramic waste forms can be tailored (i.e. unique crystalline structures) to host radionuclides by binding them into a specific crystalline network. Ceramic waste forms are tailored based on the knowledge and understanding of naturally occurring minerals containing radioactive and non-radioactive species similar to the radionuclides of concern in wastes from fuel reprocessing.

This report summarizes the data collected in support of future melter demonstration testing for crystalline ceramic waste forms. Detailed progress on processing and composition development of crystalline ceramic waste form materials is detailed in FY10, 11, and 12 reports [5-7]. This report will refine the composition and processing conditions outlined in the recent "Reference Formulation Report for Crystalline Ceramic Waste Forms"[7]. This report will form the basis of subsequent FY13 studies to select a reference ceramic and process technology for the incorporation of i) combined HLW raffinate stream (containing undissolved solids and soluble technetium) and ii) transuranic (TRU) waste stream from fuels fabrication.

2.   Reference Composition-Target vs. Achieved Phase Formation

The targeted phase composition for incorporation of the combined Cs/Sr, lanthanide fission products and transition metal waste stream (CW-AFHZ) is given in Table 2-1 [7]. Fe_2O_3 (5.82 wt %) was used as the baseline additive for improved hollandite formation. An SEM micrograph depicting the microstructure of the reference waste form (CW-AFHZ) melted at 1500^oC for 20 minutes in a $1\%H_2$ balance argon atmosphere is shown in Figure 2-1. The targeted hollandite, perovskite, and zirconolite phases were observed along with alumina, powellite, and a Cs-Mo phase. The measured phases and their compositions are summarized in Table 2-2.

Table 2-1. Reference Ceramic Composition (wt %) for CSLNTM-High Mo Waste Streams.

Fe or multivalent transition metal (Co, Zn, Cr) to assist hollandite formation[8, 9]

Composition	wt %	Targeted Phase
Waste	23.74	
Al_2O_3	6.62	*Hollandite*
TiO_2	51.03	*Hollandite, Perovskite, Zirconolite*
CaO	1.36	*Zirconolite*
BaO	11.43	*Hollandite*
*Fe_2O_3	5.82	*Hollandite*
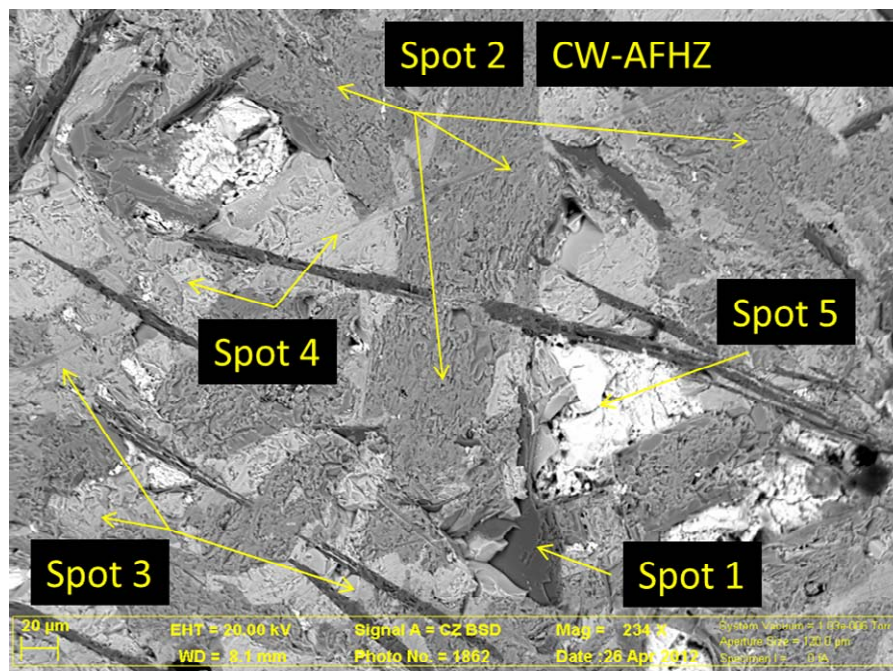
Figure 2-1.   CW-AFHZ Fabricated by a Melting and Crystallizing in a $1\%H_2$ balance Argon-Backscattered Electron Micrograph

Table 2-2. CW-AFHZ Fabricated by Melting and Crystallizing in 1%H$_2$ balance Argon-Summary of Elements and Crystalline Phases (*Crystalline phases determined from XRD measurements and EDAX elemental analysis*)

Spot	Elements (Major, Minor)	Crystalline Phases*
1	O, Al	Al$_2$O$_3$
2	O, Ti, Al,Ba	Hollandite- BaAlTi$_5$O$_{14}$
3	O,Ti, Zr,Ca	Zirconolite-CaZrTi$_2$O$_7$
4	O,Ti, Ca,Nd	Perovskite- Nd doped CaTiO$_3$
5	O, Cs, Mo, Ca, Ba	Cs$_2$MoO$_4$ + (BaCa)MoO$_4$

The successful demonstration of melt processing of ceramic waste forms achieving the targeted phases has been accomplished, however there were additional crystalline phases observed that possessed low durability, specifically the alkali molybdate phases. This is being addressed by varying the transition metal elements in the hollandite structure [9] to facilitate Cs incorporation into the hollandite structure to minimize secondary Cs-Mo phase formation and continued processing in reducing conditions using metal/metal oxide buffers such as Ti/TiO$_2$ [10].

3.   Single Phase Hollandite-Composition and Processing

Hollandite derived ceramic waste forms for immobilization of Cs have been previously melted in air using Cr, Ni, Zn or Co transition metal substitutions resulting in PCT-B normalized leachate concentrations below 0.2 g/L[9]. The present study used melt processing in air to fabricate three single phase hollandite ceramics with the following stoichiometries:

> i)   Fe-Hollandite (Ba$_1$Cs$_{0.3}$Fe$_{2.3}$Ti$_{5.7}$O$_{16}$),
> ii)   Cr-Hollandite (Ba$_1$Cs$_{0.3}$Cr$_{2.3}$Ti$_{5.7}$O$_{16}$), and
> iii)   Fe/Al/Cr-Hollandite (Ba$_1$Cs$_{0.4}$Cr$_{1.2}$Al$_{0.2}$Fe$_1$Ti$_{5.7}$O$_{16}$).

The Fe-Hollandite sample was used as a baseline composition from which to compare phase formation and Cs incorporation. The Cr- and Fe/Al/Cr- Hollandite samples were designed to promote single phase hollandite formation while simultaneously suppressing undesirable secondary phases.

In addition to compositional variants, all samples were processed with excess Ti metal and TiO$_2$ (referred to in this text as Ti/TiO$_2$ buffer). The Ti metal was added – <230 mesh, ~2.0 wt. % – to control the RedOx state during processing and in effect, phase formation. TiO$_2$ was added – ~6.5 wt. % – to buffer the reducing effects of the Ti metal on TiO$_2$. Ti metal is expected to have a localized effect as it reacts with the batch, reducing TiO$_2$ (Ti^{+4}) to a Ti$_2$O$_3$ (Ti^{+3}) and is also oxidized to Ti$_2$O$_3$ (Ti^{+3}). The reduction of Ti^{+4} to Ti^{+3} promotes hollandite formation (requiring multivalent B site species) and the oxygen partial pressure controlled by the Ti^{+4}→Ti^{+3} equilibrium maintains the overall melt conditions in a reducing regime. However, if Ti metal is added to a stoichiometric composition of hollandite, it is known to drive the material off composition by consuming TiO$_2$ (Ti^{4+}) [11]. Therefore, excess TiO$_2$ was added and anticipated as a minor phase in the single phase hollandite after synthesis.

All compositions were batched and melted in air by direct insertion of samples into a preheated furnace at 1500°C and 1600°C, held for 20 minutes at temperature, and crystallized by furnace cooling.

3.1. Fe-Hollandite ($Ba_1Cs_{0.3}Fe_{2.3}Ti_{5.7}O_{16}$)

Figure 3-1 shows the microstructure and chemical composition of Fe-Hollandite prepared without the addition of a Ti/TiO$_2$ buffer. The grains investigated exhibited the hollandite structure but, none of the examined grains contained appreciable amount of Cs. The sample displayed in **Figure 3-1** was electron irradiated and shows evidence of areas that were rendered amorphous. Energy Dispersive Spectroscopy (EDAX) chemical composition did not show any difference in chemical composition between amorphous and crystalline areas of the sample. The X-ray diffraction spectra (not shown) indicated a single phase material with the general hollandite structure ($Ba_{1.14}Fe_{2.28}Ti_{5.7}O_{16}$).

a)   b)
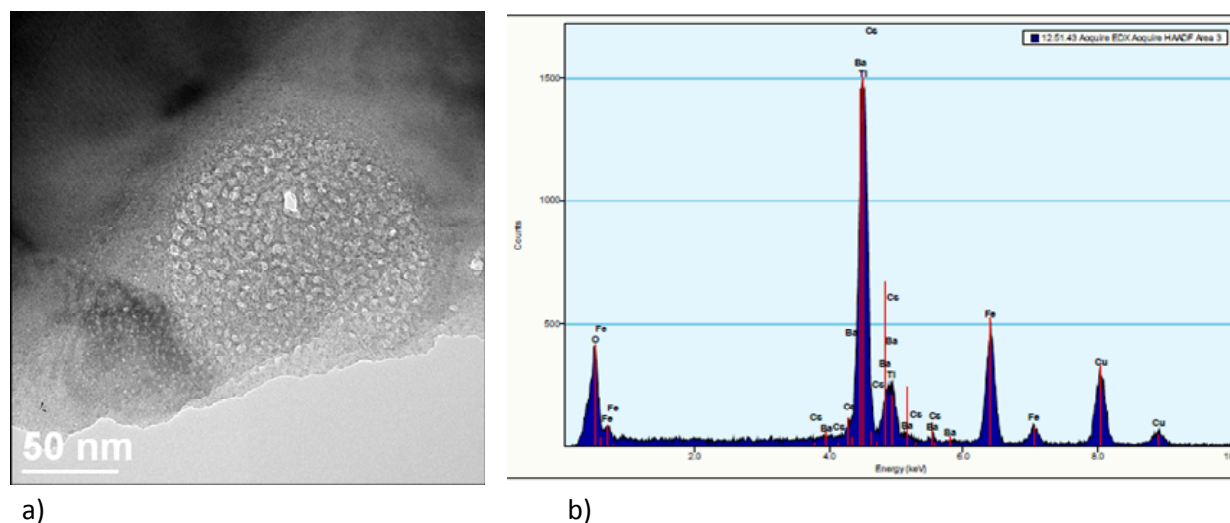
Figure 3-1. Fe-Hollandite ($Ba_1Cs_{0.3}Fe_{2.3}Ti_{5.7}O_{16}$) WITHOUT Ti/TiO$_2$ Buffer, Fabricated by Melting and Crystallizing a)TEM Bright Field Image and b) EDS Chemical Composition

The reducing conditions induced by the excess Ti/TiO$_2$ in Fe-Hollandite resulted in a multiphase crystalline assemblage as shown in Figure 3-2. The identified phases were hollandite ($Ba_{1.2}Cs_{0.28}Fe_{0.82}Al_{1.46}Ti_{5.72}O_{16}$), $Fe_3Ti_3O_{10}$ and $CsAlTiO_4$. The EDAX chemical composition revealed grains with different hollandite compositions, some containing Cs and some without Cs present along with a secondary Cs-Al-Ti phase. A comparison of Fe-Hollandite with and without excess Ti/TiO$_2$ indicated that reducing conditions seemed effective for promoting Cs incorporation into the hollandite phase. However, inhomogeneity and non-durable Cs-Al-Ti phases were also observed. Further studies are needed to understand the magnitude of composition, chemical equilibrium, and melt and crystallization processing effects on phase formation.
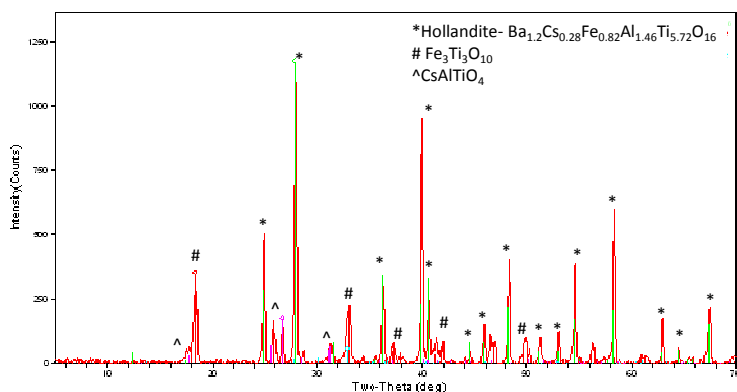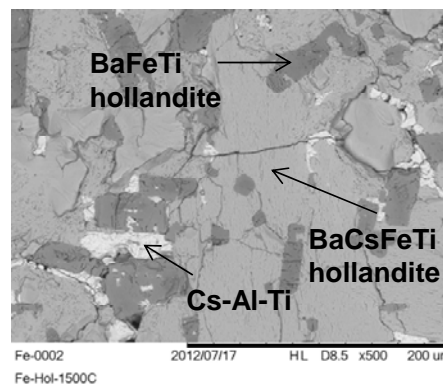
a)   b)

Figure 3-2.   Fe-Hollandite ($Ba_1Cs_{0.3}Fe_{2.3}Ti_{5.7}O_{16}$) With Ti/TiO$_2$ Buffer, Fabricated by Melting and Crystallizing a)X-Ray Diffraction Spectra and b) SEM-Backscattered Electron Micrograph

3.2.   Cr-Hollandite ($Ba_1Cs_{0.3}Cr_{2.3}Ti_{5.7}O_{16}$)

The Cr-Hollandite sample was single phase hollandite with a minor TiO_2 phase as confirmed by X-ray diffraction and EDS and shown in Figure 3-3. The chemical composition measured on different grains with EDAX identified changes in local hollandite stoichiometry, however Cs was always observed in appreciable quantities. The Cs/Ba ratio (atomic percent) was an average of ~0.5 in the areas examined which compares well with the stoichiometric value of 0.3 in Cr-Hollandite ($Ba_1Cs_{0.3}Cr_{2.3}Ti_{5.7}O_{16}$).

a)   b)
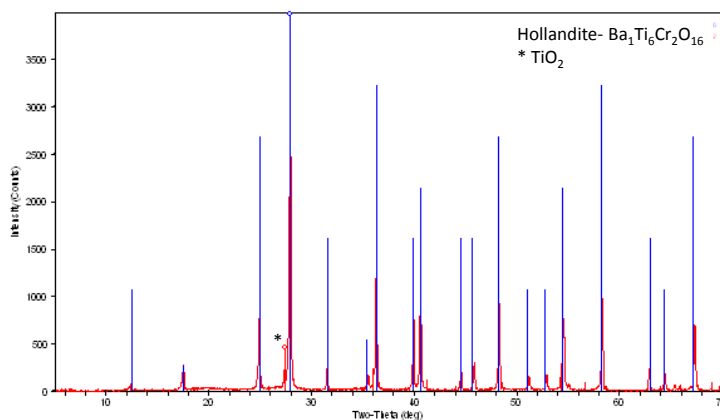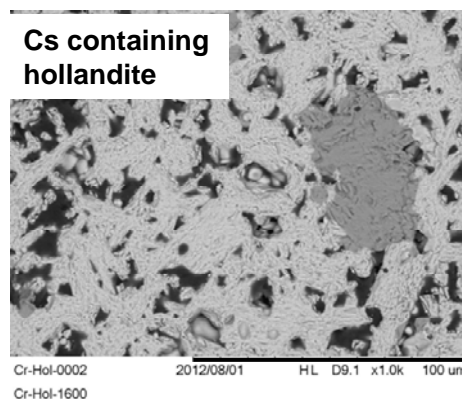
Figure 3-3.   Cr-Hollandite ($Ba_1Cs_{0.3}Cr_{2.3}Ti_{5.7}O_{16}$) With Ti/TiO$_2$ Buffer, Fabricated by Melting and Crystallizing a)X-Ray Diffraction Spectra and b) SEM-Backscattered Electron Micrograph

3.3.   Fe/Al/Cr-Hollandite ($Ba_1Cs_{0.4}Cr_{1.2}Al_{0.2}Fe_1Ti_{5.7}O_{16}$)

The Fe/Al/Cr-Hollandite sample was single phase Cs-Hollandite as confirmed by XRD and EDAX and shown in Figure 3-4 and Figure 3-5.   The chemical composition measured across different grains identified changes in local composition and although different grains appeared to have different hollandite compositions – with and without Cs – within a given grain, the compositional variation was small.

a)   b)
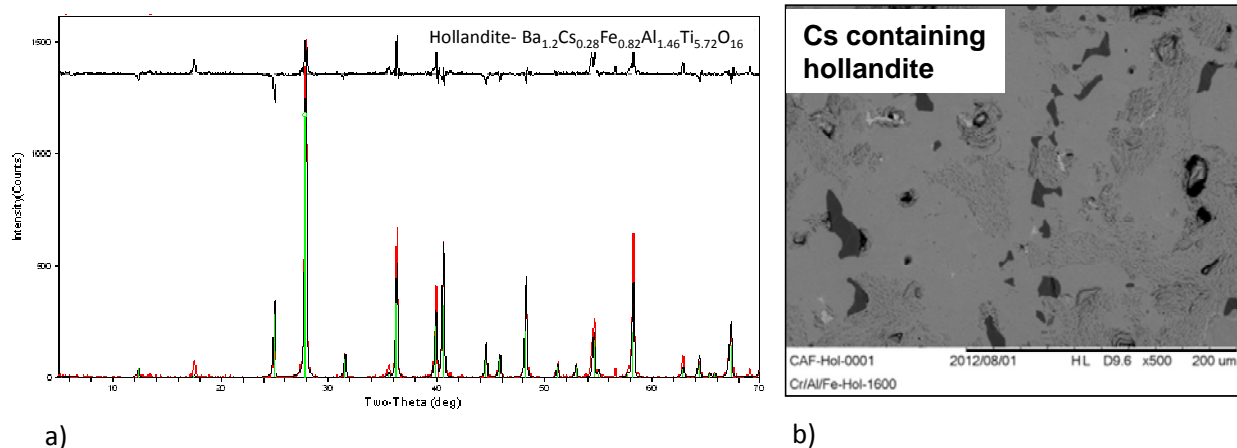
Figure 3-4.   Fe/Al/Cr-Hollandite ($Ba_1Cs_{0.4}Cr_{1.2}Al_{0.2}Fe_1Ti_{5.7}O_{16}$) With Ti/TiO$_2$ Buffer, Fabricated by Melting and Crystallizing a)X-Ray Diffraction Spectra and b) SEM-Backscattered Electron Micrograph
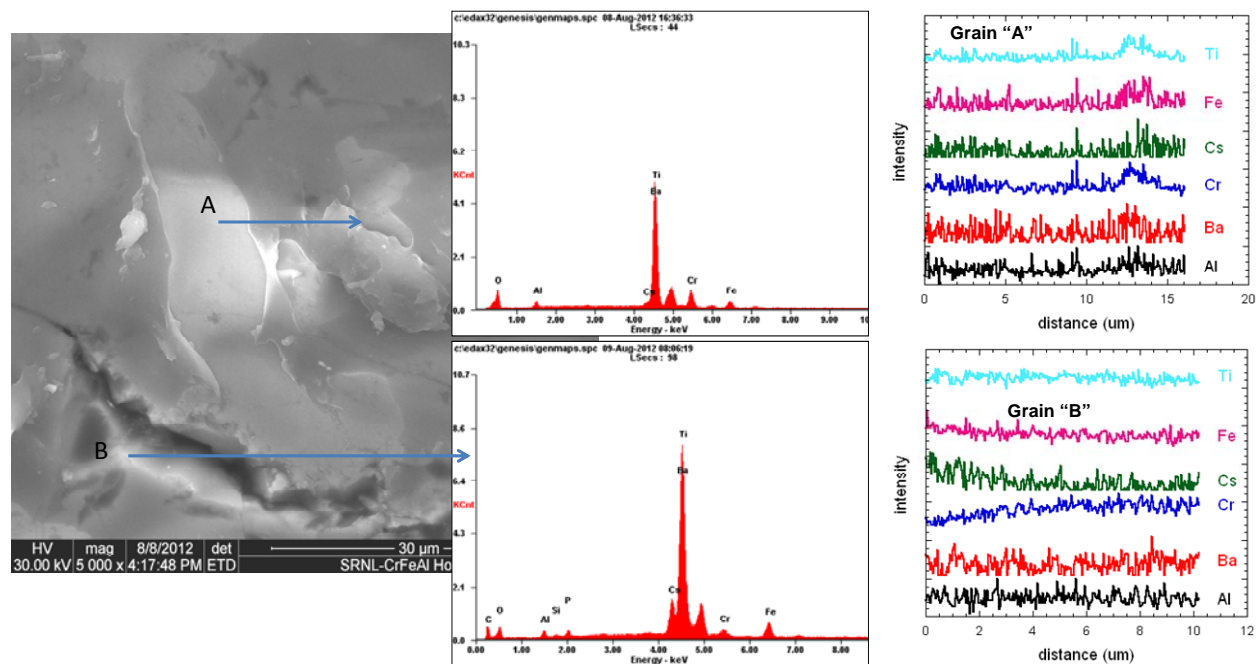
Figure 3-5.   Fe/Al/Cr-Hollandite ($Ba_1Cs_{0.4}Cr_{1.2}Al_{0.2}Fe_1Ti_{5.7}O_{16}$) With Ti/TiO$_2$ Buffer, Fabricated by Melting and Crystallizing SEM-Backscattered Electron Micrograph and Energy Dispersive Spectroscopy (EDAX) at Different Grain Locations.

In summary, substituting a portion of the Fe for Cr or a combination of Cr and Al in the target hollandite composition, along with Ti/TiO_2 buffers, resulted in single phase hollandite formation with the requisite Cs-incorporation. The path forward for this effort includes incorporating Cr-Hollandite and Fe/Al/Cr Hollandite into the multiphase waste forms and evaluating phase formation in those more complex systems.

4. Radiation Stability

Preliminary evaluations of the radiation damage tolerance of select ceramic waste forms were undertaken by subjecting samples to ion irradiations at LANL. In this study, LANL researchers used dual beam light and heavy ion bombardment, and electron irradiations to simulate the self-radiation damage that occurs in a material incorporating nuclides undergoing radioactive decay. Most of the self-irradiation in a waste form incorporating fission products is due to beta particle and gamma emission. These emissions cause radiation damage primarily via radiolytic processes, because both beta and gamma particles induce substantial electronic excitations in a target material. Light ions and electrons provide a useful means to examine radiolysis effects because they deposit nearly all of their energy in solids via electronic loss processes; and heavy ion are used to simulate energetic recoil nuclei interaction which involves ballistic processes.

4.1.   *Electron Irradiation (TEM)- Hollandite*

LANL performed a series of *in situ* electron irradiations using 300-keV electrons generated in a Tecnai F30 transmission electron microscope (TEM) in the Electron Microscopy Laboratory. By focusing electrons in the TEM on certain crystalline phases of the waste forms, it was possible to simulate radiolysis effects that might be experienced by potential crystalline ceramic waste forms.

Figure 4.1 shows the electron irradiation study for single phase Fe-Hollandite sample. High resolution TEM images and inset fast Fourier transforms (FFT) indicate Fe-Hollandite undergoes a crystalline to amorphous transition after a radiation dose of 10^{13} Gy. The results suggest that this hollandite phase materials exhibit stability to 1000 years at anticipated doses (2×10^{10}-2×10^{11} Gy)– but that their stability may be rate dependent which may limit the activity of the waste for which they can be employed.
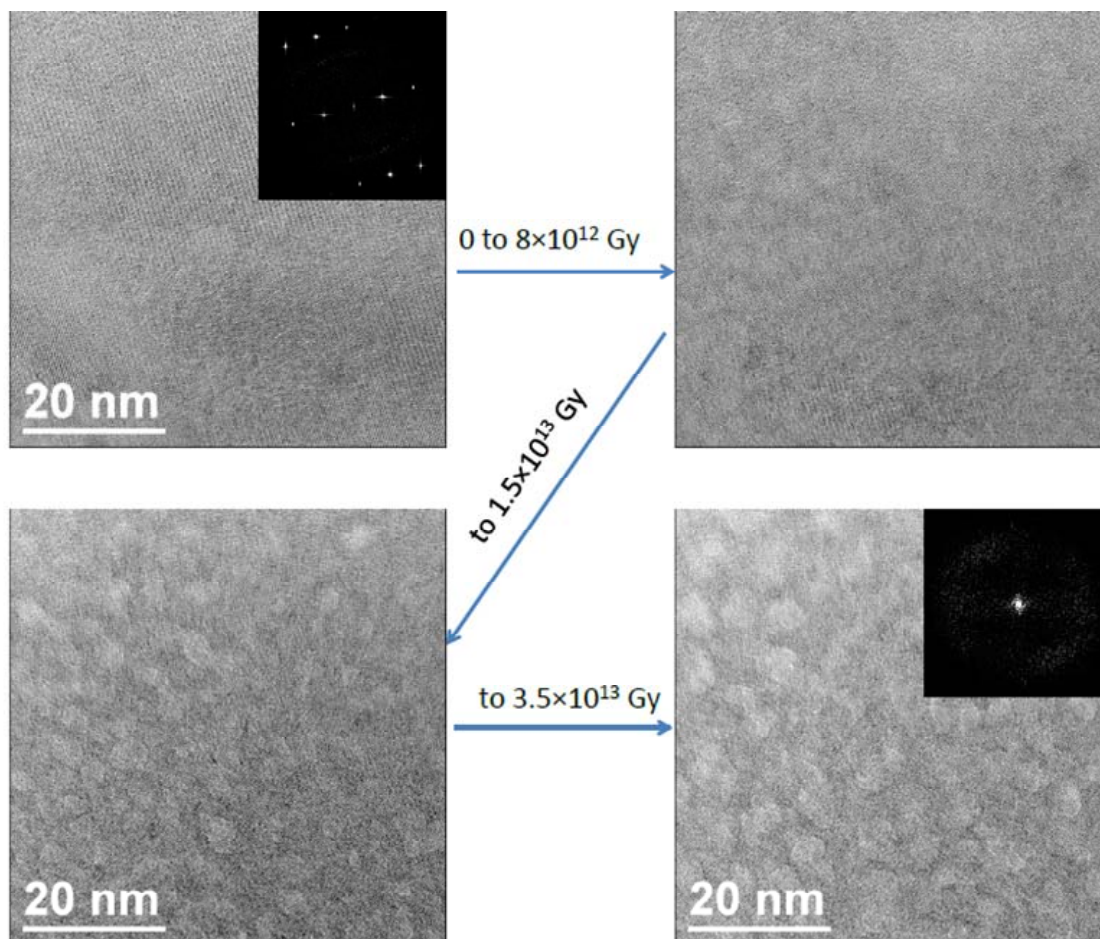
Figure 4-1. Fe-Hollandite (WITHOUT Ti/TiO$_2$ additions) High-Resolution TEM Images Reveal Change to the Crystalline Structure of the Hollandite Phase Following Electron Irradiation at the Level of 10^{13} Gy.

An additional hollandite structure was examined to confirm these results. Figure 4-2 shows the TEM determined microstructure and composition from a Al-Hollandite prepared by melt and crystallization process without Ti/TiO$_2$ buffer additions. Figure 4-3 shows high resolution TEM images indicating changes to the crystalline structure of Al-Hollandite including a crystalline to amorphous transition after a radiation dose of 10^{13} Gy. It is noted that both of the hollandite samples examined above were prepared did not have appreciable quantity of Cs incorporated into the structure.

The impact of Cs containing hollandite was also investigated using an Al/Fe-Hollandite samples presented in **Figure 4-4**. The bright field TEM and EDAX presented indicate Cs incorporation into the hollandite structure. **Figure 4-5** shows high resolution TEM images indicating changes to the crystalline structure of Cs containing Al/Fe-Hollandite including a crystalline to amorphous transition after a radiation dose of 10^{13} Gy. From these initial studies, it appears that the Cs content has little impact on the radiation stability of the hollandite structure.

a)   b)

Figure 4-2. Al-Hollandite-($Ba_1Cs_{0.2}Al_{2.3}Ti_{5.7}O_{16}$) TEM/EDX WITHOUT Ti/TiO$_2$ Buffer, Fabricated by Melting and Crystallizing a)TEM Bright Field Image and b) EDS Chemical Composition
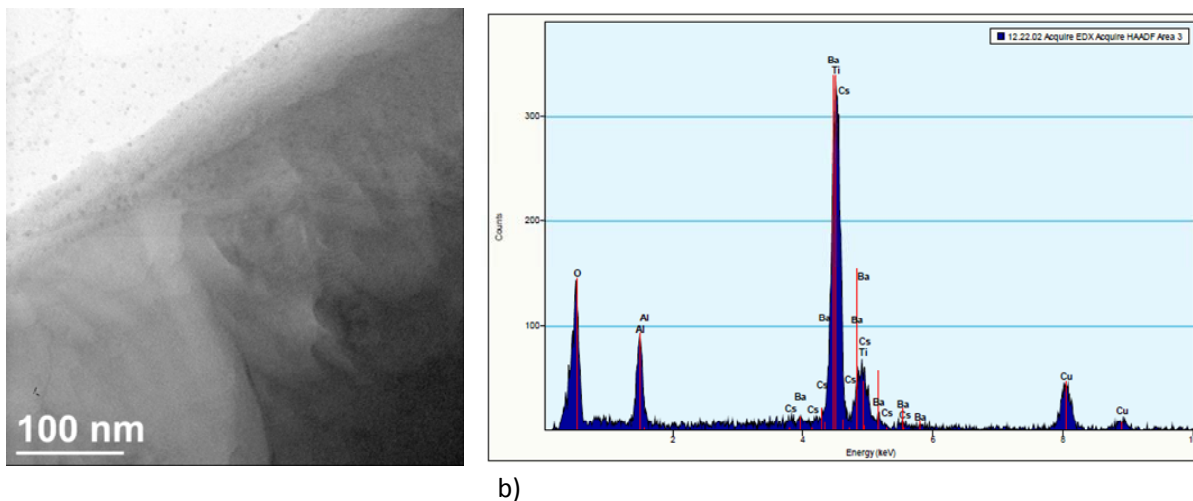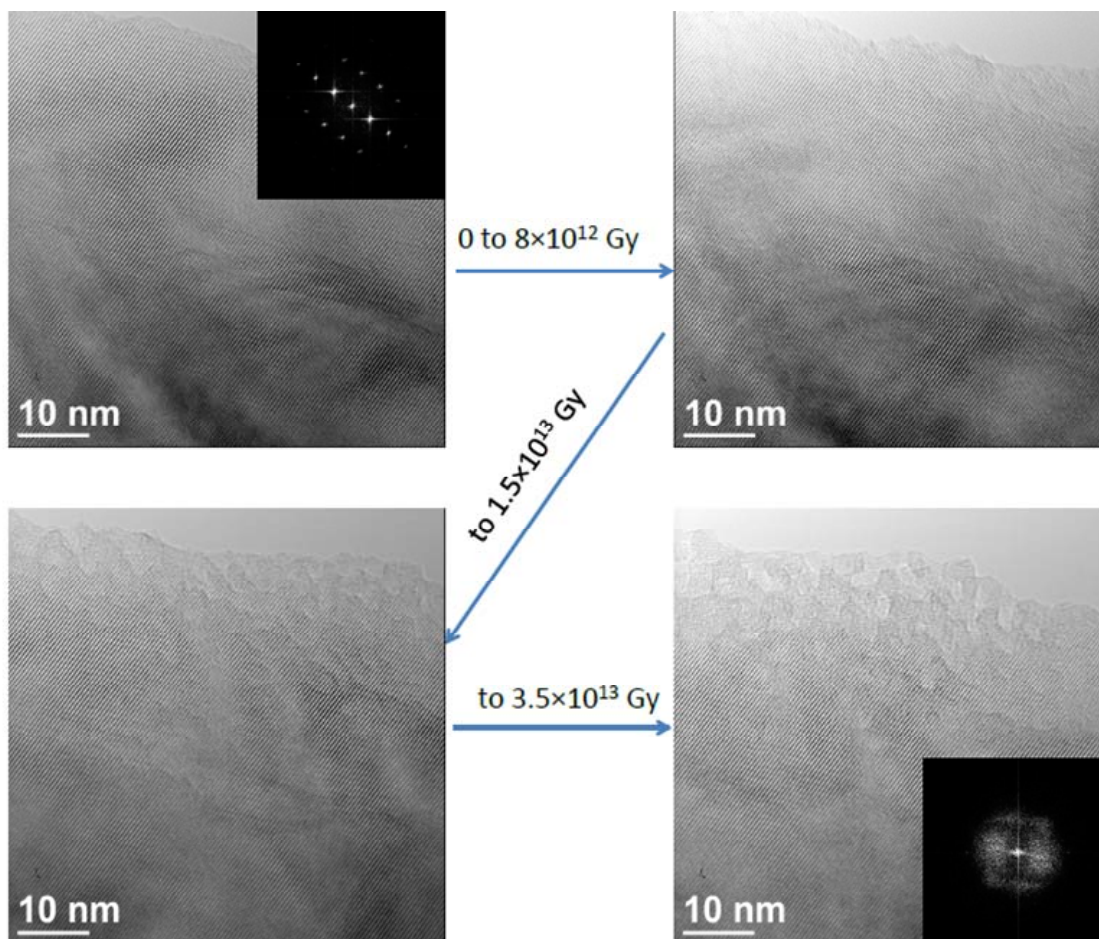

Figure 4-3.   Al-Hollandite- High-Resolution TEM Images Reveal Change to the Crystalline Structure of the Hollandite Phase Following Electron Irradiation at the Level of 10^{13} Gy.

a)   b)
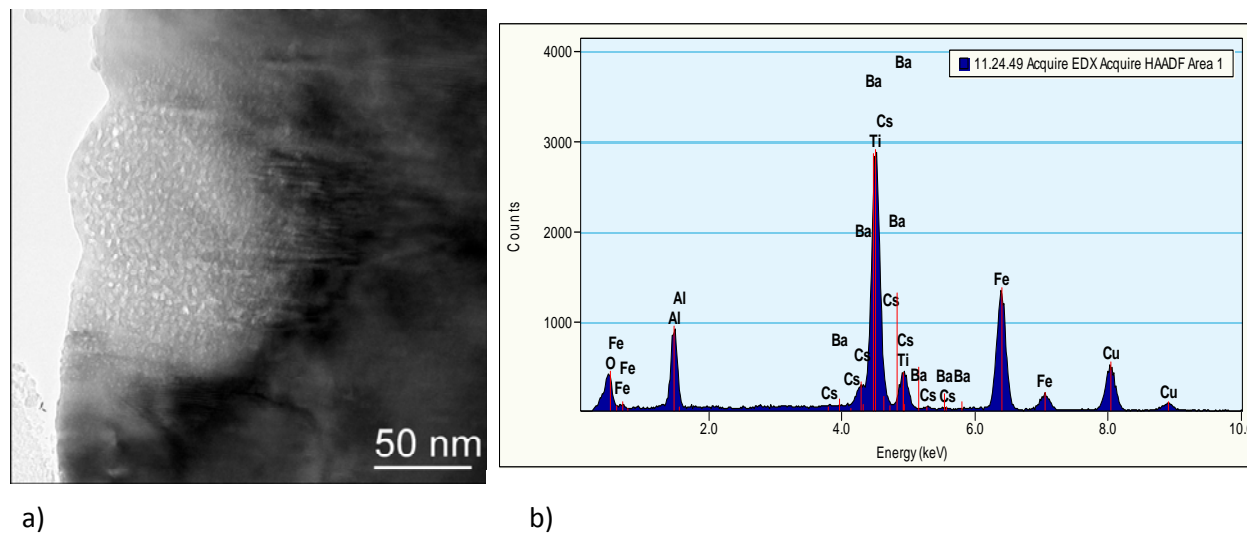
Figure 4-4. Al/Fe-Hollandite ($Ba_1Cs_{0.28}Al_{1.46}Fe_{0.82}Ti_{5.72}O_{16}$)- TEM/EDX WITHOUT Ti/TiO$_2$ Buffer, Fabricated by Melting and Crystallizing a)TEM Bright Field Image and b) EDAX Chemical Composition
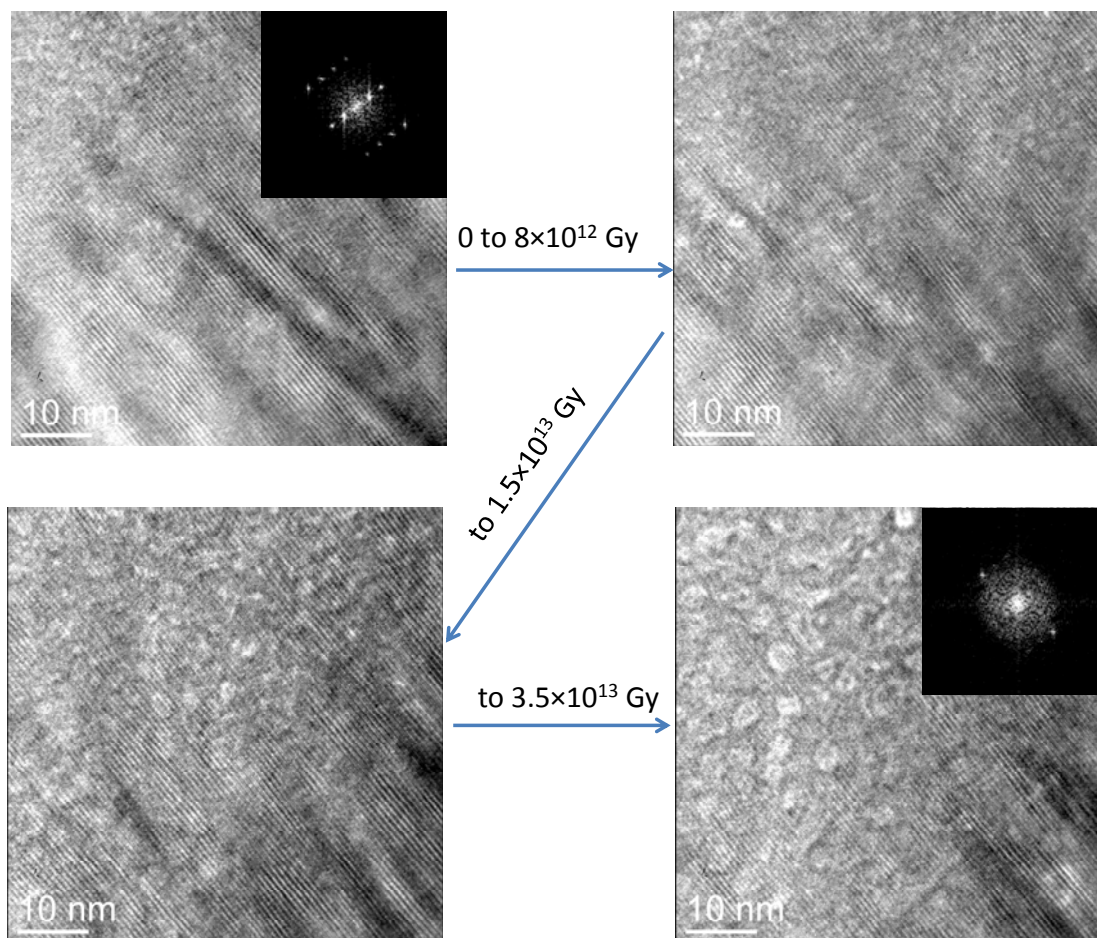
Figure 4-5.   Al/Fe-Hollandite- High-Resolution TEM Images Reveal Change to the Crystalline Structure of the Hollandite Phase Following Electron Irradiation at the Level of 10^{13} Gy.

4.2.   Dual Beam Studies- Combined Waste Forms

The principal sources of radiation in high-level nuclear wastes (HLW) are β-decay of the fission products (e.g., 137Cs and 90Sr) and α-decay of the actinide elements (e.g., U, Np, Pu, Am, and Cm). Beta-decay produces energetic β -particles, very low energy recoil nuclei, and γ-rays, whereas, α-decay produces energetic α-particles (4.5 to 5.5 MeV), energetic recoil nuclei (70 to 100 keV), and some γ-rays. Beta and alpha decay affect crystalline materials through the interactions of the β -particles, α-particles, recoil nuclei, and γ-rays with the ceramic phases. These interactions fall into two broad categories: the transfer of energy to electrons (ionization and electronic excitations) and the transfer of energy to atomic nuclei, primarily by ballistic processes involving elastic (billiard-ball-like) collisions.
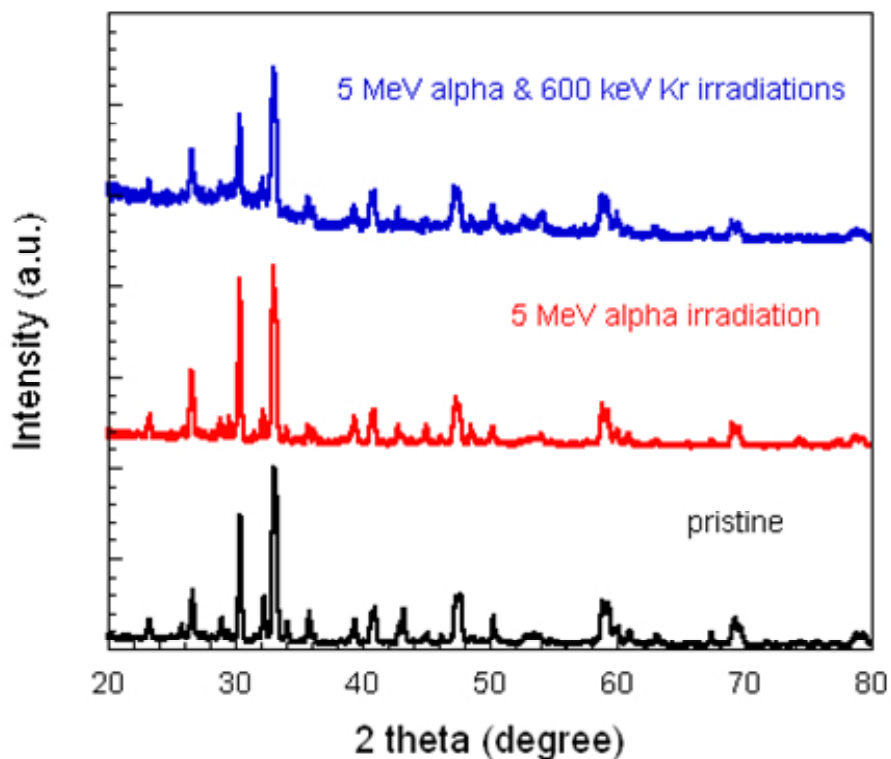
Figure 4-6.   CSLNTM-2- Dual Beam Radiation Damage: Before and After 5MeV Alpha and 600 keV Kr Room Temperature Irradiation

Dual-beam ion irradiations capability at IBML provide a useful means to examine radiation stability of advanced nuclear waste forms, because light ion beam (such as 5 MeV alpha) generated by a 3.2 MeV Tandem accelerator could be used to simulate α-particles and heavy ion beam (such as 100 keV Kr) from ion implanter used to simulate energetic recoil nuclei.

Table 4-1 shows two different ceramic waste form compositions that were investigated by dual-beam irradiation in the present study. CSLNTM-2 was a composition studied in FY11 with high waste loading resulting in perovskite, powellite, and zirconolite phase formation[12]. The CWAFHZCa100 sample was developed in FY12 and more closely resembles the reference ceramic composition with BaO and Fe_2O_3 additions targeting the hollandite phase in addition to perovskite, pyrochlore and zirconolite phases[7].

Table 4-1. Targeted Compositions (wt %) for the Ceramic Waste Forms used in Dual Beam Irradiation Studies.

Composition	CSLNTM-2	CWAFHZCa100
Waste	60	26
Al_2O_3	14	6
TiO_2	21	47
CaO	5	5.3
BaO	-	10.5
Fe_2O_3	-	5.2

The CSLNTM-2 sample was subjected to a 5 MeV alpha (He-light ion) beam with a fluence of 1×10^{17} ions/cm^2 (corresponding to a dose of 7 GGy) and 600 keV Kr (heavy ion) with a fluence of 2.5×10^{15} ions/cm^2 (corresponding to a dose of 4 dpa) sequentially at room temperature to provide preliminary insight into the radiation damage tolerance of the ceramic waste form,. The sample was evaluated by XRD before and after irradiation to identify any microstructural changes induced by ion irradiations (**Figure 4-6**). Under 5 MeV alpha irradiation, there are some differences in relative intensities among the peaks in the spectra but no changes in the phases present are apparent, indicating good radiation damage tolerance. The changes in relative intensity could be due to texturing since the spectra were collected from the polished surface of the sample, rather than crushed powders. After sequential dual beam ion irradiations (5 MeV alpha and 600 keV krypton), XRD measurement shows an apparent broad diffraction feature in the scattering angle $2\theta = 25\text{-}35°$, attributable to an amorphous structure. It indicates that a phase transformation from crystalline to amorphous occurs upon heavy ion irradiation.

Figure 4-7 shows XRD patterns obtained from a sample of composition CWAFHZCa100 before and after the dual beam irradiation at room temperature, 2 MeV proton (H-light ion) beam with a fluence of 1×10^{18} ions/cm^2 (corresponding to a dose of 1 GGy) and 600 keV Kr (heavy ion) with a fluence of 2.5×10^{15} ions/cm^2 (corresponding to a dose of 4 dpa) sequentially. Similar as the dual beam irradiated CSLNTM-02 sample, there is little differences in the relative intensities among the peaks in the spectra between the pristine and proton irradiated samples. However, after combined light and heavy ion irradiation damage, the spectra changes significantly the appearance of including several new peaks (near $2\theta = 55°$) and an increased amorphous regime (near $2\theta = 20\text{-}30°$) not present before irradiation. Overall, these dual beam irradiation results indicate that these crystalline ceramic materials are radiation tolerant to the β–particles and α-particles, but are susceptible to a crystalline to amorphous transition under recoil nuclei effects.
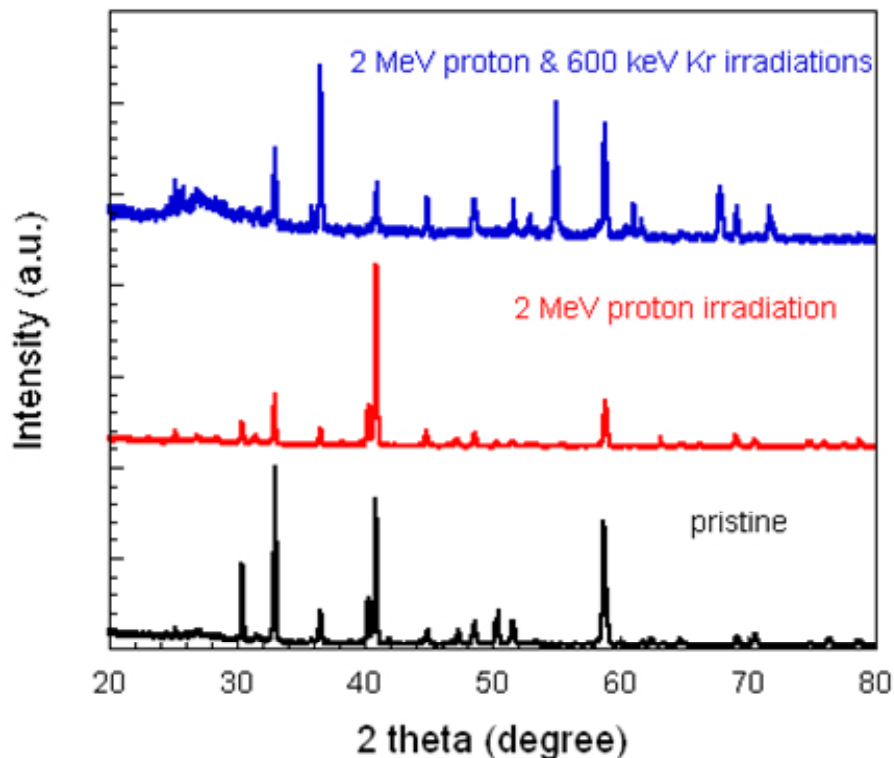
Figure 4-7. CWAFHZCa100- Dual Beam Radiation Damage: Before and After 2MeV Proton and 600 keV Kr Irradiation at Room Temperature

5. Viscosity

An examination of the viscosity of crystalline ceramic waste form melts as a function of temperature and composition is especially important when considering industrial scale melt processing. The temperature window where flow will occur as well as the critical temperature where crystallization proceeds must be determined. Figure 5-1 presents the results of initial investigations into the viscosity versus temperature relations for crystalline ceramic waste form melts. A nominal sample composition of CSLNTM-11 was chosen for initial characterization, which closely resembles the reference ceramic composition[7]. A high temperature viscometer was used with a rotating platinum alloy spindle inside a platinum alloy crucible within an electrical resistance heated furnace open to air. The sample was heated to approximately 1500 °C and the spindle was then lowered into the melt. A viscosity reading was taken after the spindle torque reading stabilized. The sample was then heated to approximately 1550 °C and a second measurement was taken. Additional measurements were taken after cooling to approximately 1450 and 1400 °C. As shown in Figure 5-1, the melt is very fluid above 1400 °C, with a relatively low viscosity that had little temperature dependence. The melt crystallized rapidly when cooled to between 1350 and 1400 °C, which locked up the viscometer and prevented further measurement. The sample was then reheated to approximately 1500 °C for a final viscosity measurement. After crystallizing and remelting, there was no change to the measured viscosity value at 1500 °C, as shown in Figure 5-1. These initial experiments indicate that the pour spout must be maintained above 1400 °C to avoid flow blockages due to crystallization for this composition. INL is currently modifying their pour spout configuration on the CCIM to address this need as part of their FY13 work scope.
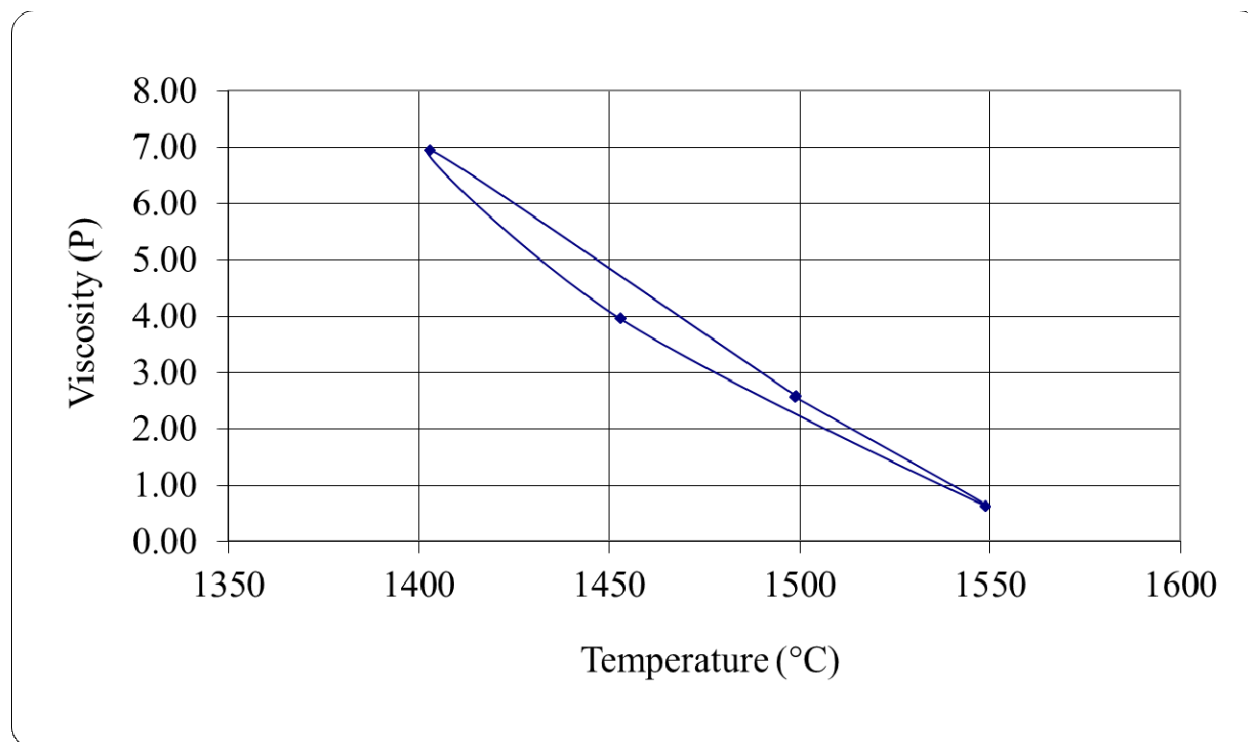
Figure 5-1. Viscosity (P) versus Temperature (^oC) for Crystalline Ceramic Waste Form

6. Path Forward

Cesium incorporation into single phase hollandite has been achieved with a melt and crystallization process using Cr transition metal and Ti/TiO$_2$ bufffer additions to control the reducing conditions. The next step is to include the refined hollandite target phase including Ti/TiO$_2$ buffer additions as part of the reference ceramic waste form composition. Initial FY13 activities will begin by targeting an alternative waste stream with lower Mo content (3% instead of 14%). This new composition will be melted in air, argon and 1%H$_2$ balance argon atmosphere. The phase formation and secondary phase content will be evaluated with particular attention paid to Cs and Mo elemental partitioning. In addition to melt processing, alternative fabrication routes are being considered including Spark Plasma Sintering (SPS) and Hot Isostatic Pressing (HIP). This work is part of collaborative activities with Alfred University as part of a DOE-NEUP program on advanced waste forms and the Australian National Nuclear Research and Development Organization (ANSTO). In addition, compositions will be developed and fabricated in FY13 with a new baseline waste stream including TRU actinide elements. The principal goal of FY13 activities remains to demonstrate both the composition and processing for incorporating combined Cs/Sr, lanthanide, and transition metal (Mo,Zr), and TRU elements into crystalline ceramic waste form with promise of higher waste loading and durability as compared to a borosilicate glass baseline

7. References

[1] Waste Forms Technology and Performance Final Report by National Research Council of the National Academies ISBN-10: 0-309-18733-8, Waste Forms Technology and Performance Final Report by National Research Council of the National Academies ISBN-10: 0-309-18733-8, (2011).

[2] J.V. Crum, L. Turo, B. Riley, M. Tang, A. Kossoy, Multi-Phase Glass-Ceramics as a Waste Form for Combined Fission Products: Alkalis, Alkaline Earths, Lanthanides, and Transition Metals, J. Am. Ceram. Soc., 95 (2012) 1297-1303.

[3] K. Brinkman, K. Fox, J.C. Marra, J. Reppert, M. Tang, J.V. Crum, Single Phase Melt Processed Powellite (Ba,Ca)MoO4 for the Immobilization of Mo-Rich Nuclear Waste, J. Alloy. Compd., Accepted (2012).

[4] A.E. Ringwood, S.E. Kesson, N.G. Ware, W. Hibberson, A. Major, IMMOBILIZATION OF HIGH-LEVEL NUCLEAR-REACTOR WASTES IN SYNROC, Nature, 278 (1979) 219-223.

[5] A.L. Billings, K. Brinkman, K.M. Fox, J.C. Marra, M. Tang, K.E. Sickafus, Preliminary Study of Ceramics for Immobilization of Advanced Fuel Cycle Reprocessing Wastes, U.S. Department of Energy Report: FCRD-WAST-2010-000158, SRNL-STI-2010-00560, Savannah River National Laboratory, Aiken, SC (2010).

[6] K. Brinkman, K.M. Fox, M. Tang, Development of Crystalline Ceramics for Immobilization of Advanced Fuel Cycle Reprocessing Wastes, U.S. Department of Energy Report: FCRD-SWF-2011-000310, SRNL-STI-2011-00516, Savannah River National Laboratory, Aiken, SC (2011).

[7] K. Brinkman, K. Fox, J.C. Marra, M. Tang, Crystalline Ceramic Waste Forms: Reference Formulation Report Report SRNL Technical Report SRNL-STI-2012-00281, FCRD-SWF-2012-000116, (2012).

[8] V. Aubin-Chevaldonnet, D. Caurant, A. Dannoux, D. Gourier, T. Charpentier, L. Mazerolles, T. Advocat, Preparation and characterization of (Ba,Cs)(M,Ti)(8)O-16 (M = Al3+, Fe3+, Ga3+, Cr3+, Sc3+, Mg2+) hollandite ceramics developed for radioactive cesium immmobilization, J. Nucl. Mater., 366 (2007) 137-160.

[9] M.L. Carter, E.R. Vance, H. Li, Hollandite-rich ceramic melts for the immobolisation of Cs, Mater. Res. Soc. Symp. Proc., 807 (2003) 249.

[10] W.J. Buykx, D.M. Levins, R.S. Smart, K.L. Smith, G.T. Stevens, K.G. Watson, D. Weedon, T.J. White, INTERDEPENDENCE OF PHASE CHEMISTRY, MICROSTRUCTURE, AND OXYGEN FUGACITY IN TITANATE NUCLEAR WASTE CERAMICS, J. Am. Ceram. Soc., 73 (1990) 1201-1207.

[11] S.E. Kesson, THE IMMOBILIZATION OF CESIUM IN SYNROC HOLLANDITE, Radioact. Waste Manage. Environ. Restor., 4 (1983) 53-72.

[12] K. Brinkman, K. Fox, M. Tang, Development of Crystalline Ceramics for Immobilization of Advanced Fuel Cycle Reprocessing Wastes, SRNL-STI-2011-00516, (2011).